Proceedings of 9th PhD Seminar on Wind Energy in Europe
September 18-20, 2013, Uppsala University Campus Gotland, Sweden

AERODYNAMIC DAMPING OF NONLINEARILY WIND-EXCITED WIND TURBINE BLADES

P. van der Male[1], K.N. van Dalen[2], A.V. Metrikine[2]
[1]Offshore Engineering, Delft University of Technology
[2]Structural Mechanics, Delft University of Technology
Delft, the Netherlands
e-mail: p.vandermale@tudelft.nl

ABSTRACT

This paper presents the first step of the derivation of an aerodynamic damping matrix that can be adopted for the foundation design of a wind turbine. A single turbine blade is modelled as a discrete mass-spring system, representing the flap and edge wise motions. Nonlinear wind forcing is applied, which couples the degrees of freedom. The structural response is determined by means of a Volterra series expansion. The contribution of the aerodynamic damping to the structural response is determined by comparing the response without structural feedback to the response that includes structural feedback.

The reduction of the structural response due to aerodynamic damping is significant. This also applies for the edge wise response and the cross response that results from the coupling. Due to the nonlinear forcing, higher order harmonics are excited. This study only presents the response to a single harmonic 1P forcing. To fully understand the response to the nonlinear forcing, a representative excitation spectrum needs to be adopted.

INTRODUCTION

In determining the wind forcing on a wind turbine, the interaction between the air flow and the structure cannot be neglected. The effective force due to a flow on a structure depends on the relative velocity of this flow with respect to the structure. If the structure responds dynamically, the relative flow velocity is affected by the structural vibration. This aspect is of particular importance for flexible structures like wind turbines, where the motion of the structure generally leads to a reduction of the effective wind force. Moreover, turbine blades are highly sensitive to perturbations in the angle of attack of the wind flow, reducing or increasing the forcing on the structure. The force reduction due to the structural feedback velocity is commonly known as added damping, or – specifically for wind turbines – as aerodynamic damping.

Complex models, making use of computational fluid-dynamics techniques, can be adopted to estimate the effective forcing – and so the aerodynamic damping – of a wind flow on a wind turbine. For early design stages this approach is time-consuming, in both model construction and calculation processing. Besides, such complex models do not necessarily provide the physical insight that can be employed to improve the aero-elastic performance of the structure. On the other hand, when it comes to foundation design, the available techniques to determine the reduction in aerodynamic forcing due to structural response are rather simplified. Linearized expressions, neglecting the dependency of the force on the mean wind speed and the coupling between flap and edge wise blade motion – among other things, are adopted to estimate the effective wind forcing [1, 2, 3]. For offshore wind turbines, the aerodynamic damping of hydrodynamic forces is recognized [4], but the existing theories do not allow for a misalignment between the aerodynamic and hydrodynamic forcing.

This paper presents the first step in the derivation of an aerodynamic damping matrix that particularly serves the design of offshore wind support structures under combined wind and wave loading. A single blade is modelled as a mass-spring system representing the flap and edge wise motions. The blade is excited by a drag force that depends quadratically on the effective flow velocity. The forcing ensures coupling between the degrees of freedom. The modelling includes dependencies on the mean wind velocity and the pitch angle of the blade. In order to account for the nonlinear character of the loading, a Volterra series expansion is applied, a technique that enables the identification of higher-order transfer kernels in the frequency domain [5].

Validation of the proposed model is performed on the basis of the NREL 5.0 MW blade characteristics [6]. First order transfer functions are compared to the transfer function that result from the existing techniques to evaluate aerodynamic damping. The second order response is analyzed for a 1P harmonic loading.

DISCRETE BLADE MODEL

A discrete model with two degrees of freedom - representing a single blade - is adopted to analyze the wind-structure interaction. Figure 1 depicts the mass-spring system, where Figure 1(a) presents the mass-spring representation of the blade as a part of the rotor. The actual mass-spring system, Figure 1(b), consists of x and y springs representing the generalized flap and edge wise blade stiffness k_x and k_y, x and y dashpots representing the generalized structural damping c_x and c_y, and generalized masses m_x and m_y. Generalization is done on the basis of the undamped first flap and edge wise fixed interface modes of vibration. The application of fixed interface modes implies that the blade is assumed clamped at its root and that tower flexibility is not accounted for. The flap wise deflection is given by u_x, while u_y expresses the edge wise motion. The angle β represents the pitch angle with which the aerodynamic blade response can be controlled.

The system of equations describing the dynamic behaviour of the blade model can be written as:

$$\mathbf{M}\ddot{\vec{u}} + \mathbf{C}\dot{\vec{u}} + \mathbf{K}\vec{u} = \vec{f} \tag{1}$$

, where

$$\mathbf{M} = \begin{bmatrix} m_x & 0 \\ 0 & m_y \end{bmatrix}; \quad \mathbf{C} = \begin{bmatrix} c_x & 0 \\ 0 & c_y \end{bmatrix}; \quad \mathbf{K} = \begin{bmatrix} k_x & 0 \\ 0 & k_y \end{bmatrix};$$
$$\vec{u} = \begin{bmatrix} u_x \\ u_y \end{bmatrix} \tag{2}$$

The forcing vector consists of an x and y component:

$$\vec{f} = \begin{bmatrix} f_x \\ f_y \end{bmatrix} \tag{3}$$

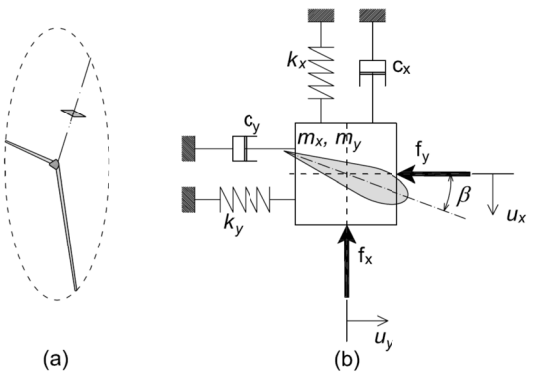

Figure 1: (a) the mass-spring representation of the blade as a part of the rotor, (b) discrete model with two degrees of freedom, representing a single blade.

AERODYNAMIC FORCING

Since the blade is modelled using the generalized coordinates u_x and u_y, the forcing vector $\vec{f}$ represents a generalization too. This generalization can be expressed as:

$$\vec{f} = \int_0^R \boldsymbol{\mu}\,\hat{\vec{f}}\,dr \tag{4}$$

, where $\hat{\vec{f}}$ represents the distributed aerodynamic forcing vector – consisting of the force components in x and y direction $\hat{f}_x$ and $\hat{f}_y$ – and $\boldsymbol{\mu}$ the matrix containing the first flap and edge wise fixed interface modes of vibration μ_{x1} and μ_{y1} on its main diagonal, whereas the off-diagonal entries are zero. Both components are a function of the radius r and in order to obtain the generalized forcing vector, the product needs to be integrated over r.

In order to define the wind load on the blade the following nonlinear flow-force relation is adopted:

$$\hat{\vec{f}} = \tfrac{1}{2}\rho A(\mathbf{C_a}\boldsymbol{\Psi})^{\mathrm{T}}\vec{w}|\vec{w}| \tag{5}$$

This relation defines the force vector $\hat{\vec{f}}$ as a quadratic function of the relative flow velocity $\vec{w}$, which consists of the mean flow $\vec{\bar{v}}$, the flow fluctuation $\vec{v}$ and the structural feedback velocity $\hat{\dot{\vec{u}}}$:

$$\vec{w} = \vec{\bar{v}} + \vec{v} - \hat{\dot{\vec{u}}} \tag{6}$$

Like for the forcing vector $\vec{f}$, the hat on $\vec{u}$ indicates spatial dependency. All components of $\vec{w}$ can be radius-dependent. Figure 2 depicts the flow vector $\vec{w}$ that excites the blade model. Within the frame of reference, x and y components of the flow vector can be distinguished. $\bar{v}_x$ represents the mean wind velocity that acts on the blade, whereas $\bar{v}_y$ is the constant tangential velocity of the rotating blade. It is assumed that the y component of the mean wind velocity is zero. For an idling turbine, $\bar{v}_y$ equals zero. v_x and v_y represent fluctuations of the wind field. The distributed structural feedback velocity $\hat{\dot{\vec{u}}}$ can be represented by the matrix-vector product of the matrix $\boldsymbol{\mu}$ and the generalized structural response velocity vector $\dot{\vec{u}}$.

Other components of (1) are the air density ρ, the blade chord width A, and the blade aero-elastic matrix $\mathbf{C_a}$, which consists of the lift and drag coefficients C_L and C_D:

$$\mathbf{C_a} = \begin{bmatrix} C_L & 0 \\ 0 & C_D \end{bmatrix} \tag{7}$$

The wind flow $\vec{w}$, being active under an angle φ with respect to the rotor plane, results in a lift and drag force $\vec{f}_L$ and $\vec{f}_D$, see

Figure 2. In order to obtain force components in x and y direction, the transformation matrix $\mathbf{\Psi}$ is applied:

$$\mathbf{\Psi} = \begin{bmatrix} \cos\varphi & \sin\varphi \\ \sin\varphi & -\cos\varphi \end{bmatrix} \quad (8)$$

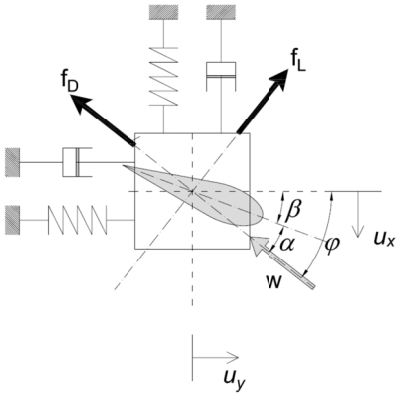

Figure 2: air flow excited blade model and resulting lift and drag forces.

The generalized forcing vector $\vec{f}$ follows from integration over the blade length. Therefore, an important aspect is the definition of the length depending components of (1). First of all, the mean wind velocity $\bar{v}_x$ is assumed to be constant within the blade swept area. The same applies for the wind fluctuations v_x and v_y. For the tangential velocity $\bar{v}_y$ a linear radius dependent function is adopted, which relates the velocity at radius r to the blade tip speed.
The aero-elastic coefficients $C_L$and C_D are functions of the angle of attack α, see Figure 2. These functions are assumed to be radius invariant. The only remaining component with length dependency is the chord width A.

NONLINEAR BLADE ANALYSIS

The structural response to the nonlinear excitation, which moreover forces a coupling between the responses in x and y direction, is estimated with the help of a Volterra series expansion. With the help of this technique, the nonlinear effects can be accounted for by higher-order transform kernels. Moreover, the technique permits analyses in the frequency domain. The theory is already applied in analyzing responses of wind, and combined wind and wave excited structures [7, 8]. When limiting the expansion to the second order, the frequency-domain response vector $\vec{U}$, representing the Fourier transform of $\vec{u}$ and consisting of the components U_x and U_y, can be found from the following relations:

$$\vec{U} = \vec{U}_1 + \vec{U}_2 \quad (9)$$

, where the components of $\vec{U}_1$ and $\vec{U}_2$ represent the first- and second-order frequency responses. The first-order response follows from the well-known linear relation, where the input-output relation is defined by the transfer function matrix $\mathbf{H_1}$:

$$\vec{U}_1 = \mathbf{H_1}\vec{V} \quad (10)$$

The vector $\vec{V}$, representing the Fourier transform of $\vec{v}$, consists of the frequency dependent excitation signals V_x and V_y, the matrix $\mathbf{H_1}$ contains direct- and cross-kernel transforms, or direct or cross frequency-response functions. The second-order Volterra kernels are not just a function of the excitation frequency ω, but of the frequency ω_1 too. In order to find the second-order response $\vec{U}_2$, the direct- and cross-kernel transforms, combined in the 2×4 matrix $\mathbf{H}_2$ need not only be multiplied by the excitation signal $\vec{V}^*$, but as well by the excitation signal $\vec{\bar{V}}^*$. Moreover, the relation needs to be integrated with respect to ω_1 over an infinite interval:

$$\vec{\mathbf{U}}_\mathbf{2} = \frac{1}{2\pi}\int_{-\infty}^{\infty} \mathbf{H}_2\, \vec{V}^*\vec{\bar{V}}^{*\,\mathbf{T}}\, d\omega_1 \quad (11)$$

The asterisks imply double entries of V_x and V_y, to maintain consistency with the $\mathbf{H}_2$ matrix. The entries of the vector $\vec{V}^*$ are functions of ω, while the entries of $\vec{\bar{V}}^*$ are functions of $(\omega - \omega_1)$.

Identification of the Volterra kernels can be achieved by applying the harmonic probing algorithm [9]. An elegant alternative exists in assembling complicated kernels from known partial solutions [10].Since the harmonic probing algorithm has already been extended for multi-input and multi-output systems [11], this approach is adopted for the current Volterra kernel identification.

It can easily be shown that the first order Volterra kernels represent the frequency-response function for the linearized system. Higher-order Volterra kernels cannot be defined as unique frequency response functions, but are input-dependent.

LINEARIZED BLADE RESPONSE

Currently, aerodynamic damping due to blade motion is estimated using one-degree-of-freedom systems as a result of linearized wind flow-structure interaction. According to this approach, which is only valid for operating turbines, the flap wise motion of the blade results from the tangential velocity of the rotating blade only. Small fluctuations in the wind field, and the flap wise feedback velocity, cause perturbations in the flow angle and therefore in the lift coefficient. Based on this, an expression for the aerodynamic damping can be obtained, which among other things, neglects the mean wind velocity, the pitch angle and the coupling of flap and edge wise motion.

NREL 5.0MW BLADE ANALYSIS

The structural response to the nonlinear wind-flow excitation is determined for a single blade of the NREL 5.0 MW reference turbine [6]. For convenience's sake, the edge wise structural properties have been related in a simple manner to the flap wise characteristics, namely $m_x = m_y = 2242$ kg and $k_x = \frac{1}{2}k_y = 13141$ N/m. It should be noted that an increase in

effective stiffness due to the rotation of the blade has not been accounted for. The natural frequencies corresponding to the motions are 2.42 rad/s and 3.42 rad/s. For structural damping a damping ratio of 0.01 is adopted.

The geometry of the blade is defined by its radius 63 m and the chord width, for which a radius independent average value of 3.0 m is adopted. The blade angle β is set at 0°, the rated tip speed is 80 m/s, and the mean wind velocity is 15 m/s. In order to define the generalized forcing, modal shapes proportional to a simplified expression for cantilever beams, $\mu_{x1} = \mu_{y1} = 1 - cos\left(\frac{\pi}{2}\frac{r}{R}\right)$, are applied.

In order to derive first- and second-order Volterra kernels from the system described by equation (1-8), a number of assumptions have been adopted:

- The magnitude of the constant contribution to the relative flow $\vec{w}$ is larger than that of the fluctuating parts, i.e $|\vec{v}| > |\vec{v} - \hat{\vec{u}}|$. Moreover, the vector that follows from the multiplication $\vec{w}|\vec{w}|$ is replaced by a vector with the two equal entries $(w_x^2 + w_y^2)$.
- The blade remains unstalled, implying that the contribution of the drag force $\vec{f_D}$ can be neglected and the relation between the lift coefficient C_L and the angle of attack α is linear.
- The local blade twist angle β is constant in time.
- Trigoniometric operations of the flow angle φ can be approximated by the first term of the Taylor expansion around $\varphi = 0$.
- The time-dependent contributions to the y component of the relative flow $\vec{w}$ - v_y and $\hat{u}_y$ – do not affect the fluctuation of the flow angle φ.

In comparison with the linearized approach, defined by the equation (13-15), the mean wind velocity, pitch angle and radius dependent tangential velocity have been taken into account explicitly. Moreover, coupling between flap and edge wise motion has been adopted and the quadratic flow-structure interaction has been accounted for by incorporating second-order Volterra kernels.

Figure 3 presents the linear direct and cross frequency-response functions of the nonlinear blade model, when neglecting the structural feedback $\vec{u}$, see (6). Large peaks at the natural frequencies can be observed. The contribution of the cross-terms is significant; the response U_y is mostly affected by fluctuations of V_x. To verify the results, the transfer function of the linearized system is plotted too. Due to the fact that the pitch angle is set at 0°, this curve precisely follows the response U_x to fluctuations of V_y.

By taking system feedback into account, the picture presented by Figure 3 gets disturbed, as can be seen in Figure 4. First of all, the height of the peaks has significantly decreased, which can be seen as the result of the added damping. Moreover, system response in u_x direction affects the u_y response, and vice versa.

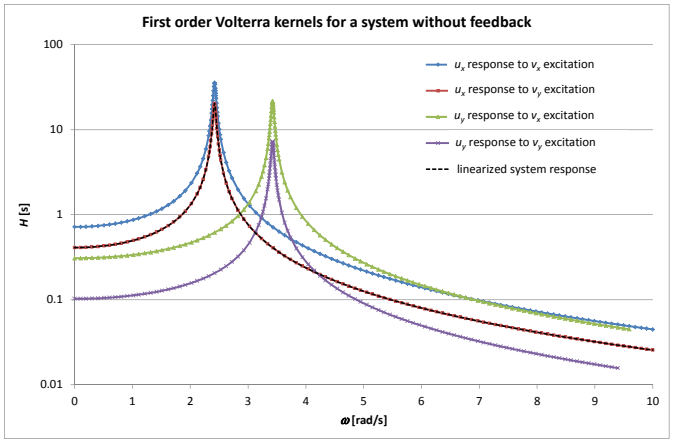

Figure 3: First-order Volterra kernels, or frequency response functions, of the blade model without system feedback. Note the linearized system response, which equals the u_x response to v_y excitation.

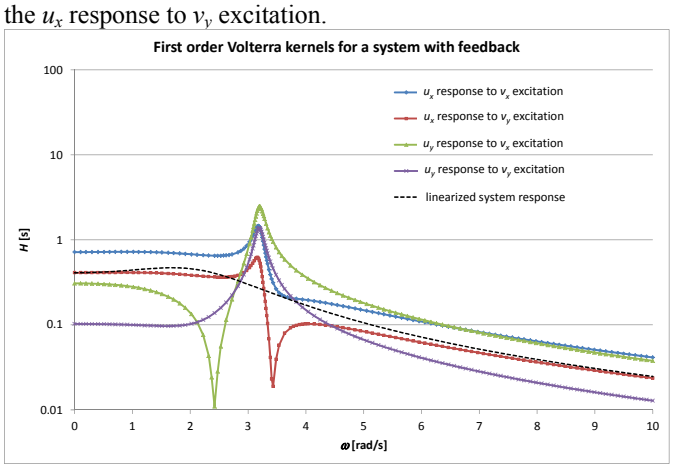

Figure 4: First-order Volterra kernels, or frequency-response functions, of the blade model with system feedback.

In order to provide insight in the contribution of the aerodynamic damping, Table 1 presents the values of the transfer functions – with and without structural feedback – at the natural frequencies and the ratios of the magnitude of the transfer functions. The effect of the structural feedback is most significant for the flap wise response. The flap wise reduction ratios are in line with the ratio obtained with the linearized model. For the given configuration, the aerodynamic damping affects the structural response in y direction much less.

	No feedback [s]	Feedback [s]	Ratio [-]
U_x response to V_x excitation	35.8	0.651	55.0
U_x response to V_y excitation	20.4	0.365	55.9
U_y response to V_x excitation	21.7	0.977	22.2
U_y response to V_y excitation	7.22	0.476	15.2
Linearized system response	20.4	0.405	50.4

Table 1: Transfer function values at natural frequencies, with and without structural feedback.

Until now, only first-order responses have been considered. To analyze also the second-order response, which accounts for the nonlinearity of the system excitation, a specific forcing needs to be defined, since the second order Volterra kernels do not provide input independent transfer functions in the frequency domain, as was obtained for the first order Volterra kernels.

As system excitation, a harmonic fluctuation corresponding to a 1P frequency (0.84 rad/s) of the turbine blade is adopted. This excitation is thought to be active both in- and out-of-plane of the rotor, with equal amplitude in both directions. The structural response for the system with and without structural feedback is depicted in Figure 5. The first-order Volterra kernels provide system response at the excitation frequency. As expected, the second-order kernel gives a response that contains higher harmonics, the response frequency of which exactly doubles the excitation frequency. The effect of the added damping can be deduced from Figure 5 too. For each line, the higher data point indicates the structural response without the added damping. The lower data point shows the response including the beneficial effect of structural feedback.

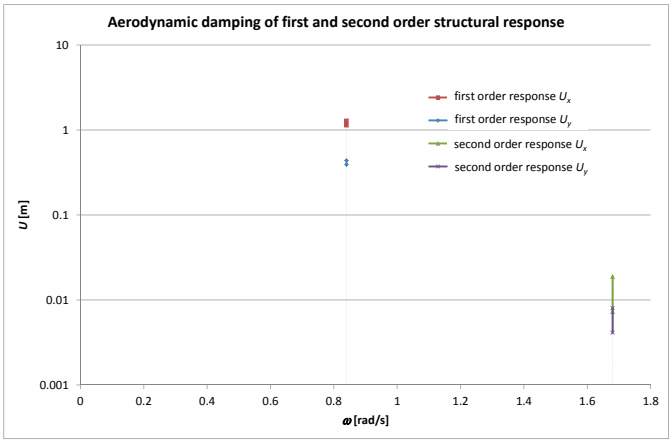

Figure 5: First and second-order structural response due to harmonic in- and out-of-plane system excitation, corresponding to the rotation frequency of the blade.

To draw sound conclusions with respect to the aerodynamic damping, the frequency response to a representative wind power spectrum should be analyzed, since this provides real insight in the actual effect on the nonlinearity of the excitation to the response at different frequencies. The derivation of an excitation spectrum, containing additional peaks due to the harmonics of the rotating turbine will be the next step in this analysis.

CONCLUSIONS

The analysis performed on the basis of the discrete blade model show the significant impact of structural feedback on the response to fluctuations in the flow field. Moreover, the importance of coupling of the flap and edge wise motions has been observed, since the cross contributions to the structural response cannot be neglected. Studying the effect of nonlinear excitation by means of second-order Volterra kernels has shown some higher-harmonic response. In order to get a clear picture of how the nonlinear forcing affects the structural motion, the response to a realistic excitation spectrum for a rotating turbine needs to be analyzed.

ACKNOWLEDGEMENTS

This work has been financially supported by the Far and Large Offshore Wind (FLOW) innovation program.

REFERENCES

[1] Burton, T., Jenkins, N., Sharpe, D. and Bossanyi, E., 2011. *Wind energy handbook*, second edition. Wiley, West Sussex, UK.

[2] Cerda Salzmann, D. and Van der Tempel, J., 2005. “Aerodynamic damping in the design of support structures for offshore wind turbines”. In *Proceedings of the Offshore Wind Energy Conference*, Copenhagen, Denmark.

[3] Garrad, A.D., 1990. “Forces and dynamics of horizontal axis wind turbines”. In Freris, L.L., editor, *Wind Energy Conversion Systems*, chapter 5, pages 119-144. Prentice Hall, Englewood Cliffs, New Jersey.

[4] Kühn, M.J., 2001. *Dynamics and Design Optimisation of Offshore Wind Energy Conversion Systems*. PhD thesis, Delft University Wind Energy Research Institute.

[5] Rugh, W.J., 1981. *Nonlinear system theory.* The John Hopkins University Press, Baltimore, Maryland.

[6] Jonkman, J., Butterfield, S., Musial, W., and Scott, G., 2009. *Definition of a 5-MW reference wind turbine for offshore system development*. Technical Report NREL/TP-500-38060, National Renewable Energy Laboratory, Golden, Colorado.

[7] Kareem, A., Tognarelli, M.A., Gurley, K.R., 1998. “Modeling and analysis of quadratic term in the wind effects on structures”. *Journal of Wind Engineering and Industrial Aerodynamics*, p. 1101-1110.

[8] Kareem, A., Zhao, J., Tognarelli, M.A., 1995. “Surge response statistics of tension leg platforms under wind and wave loads: a statistical quadratization approach”. *Probabilistic Engineering Mechanics, **10***, p. 225-240.

[9] Bedrosian, E. and Rice, S.O., 1971. “The output properties of Volterra systems (nonlinear systems with memory) driven by harmonic and Gaussian inputs”. *Proceedings of the IEEE, **59***(12), p. 1688-1707.

[10] Carassale, L. and Kareem, A., 2010. “Modeling nonlinear systems by Volterra series”. *Journal of Engineering Mechanics*, ***136***, p. 801-818.

[11] Worden, K., Manson, G., and Tomlinson, G.R., 1997. “A harmonic probing algorithm for the multi-input Volterra series”. *Journal of Sound and Vibration*, ***201***(1), p. 67-84.